CHAPTER 17

EMISSION (^{57}Co) MÖSSBAUER SPECTROSCOPY: BIOLOGY-RELATED APPLICATIONS, POTENTIALS, AND PROSPECTS

ALEXANDER A. KAMNEV

Laboratory of Biochemistry, Institute of Biochemistry and Physiology of Plants and Microorganisms, Russian Academy of Sciences, Saratov, Russian Federation

17.1 INTRODUCTION

The traditional absorption variant of Mössbauer spectroscopy, with the stable ^{57}Fe isotope most widely used up to now, has had a very rich history of applications in a broad range of biology-related and biomedical fields, which started soon after Rudolf Mössbauer's discovery. (Some earlier and more recent related representative publications are reviewed in Chapter 13[1].) For the ^{57}Fe absorption variant of Mössbauer spectroscopy, the well-known main methodological limitations are (i) a relatively low abundance of ^{57}Fe in the natural iron (2.19%), so that samples to be studied containing only traces of Fe have to be enriched with ^{57}Fe, and (ii) a relatively low sensitivity (i.e., with minimal sample requirements of over 1 mM ^{57}Fe and a sample volume about 0.3–0.4 ml [2]). As the Mössbauer effect (i.e., recoilless absorption or emission of γ-quanta) with a noticeable probability can generally be observed in a solid matrix only, solutions or liquid samples are commonly studied in a rapidly frozen state [3]. This methodology also allows 'time-resolved' Mössbauer spectra to be obtained down to a millisecond time scale (using the rapid freeze-quench method [2]). Upon rapidly freezing a solution at a certain time point, which allows its structure to be conserved [3], virtually all ongoing (bio) chemical processes in the system under study abruptly cease. Thus, a further Mössbauer study of the frozen system provides its 'snapshot' at the moment of freezing.

The emission variant of Mössbauer spectroscopy (EMS; with the ^{57}Co radionuclide as the most widely used isotope) is incomparably more sensitive and potentially very informative (for earlier and more recent reviews on or including EMS-related topics see, for example, Refs. 4–10). It requires ca. 10^3–10^4-fold lower amounts of ^{57}Co in a sample under study (which, in this case, is used as a source of γ-radiation), as compared with the ^{57}Fe absorption variant. Thus, with the theoretical specific activity of ^{57}Co of 8.5 Ci mg^{-1} (ca. 0.48 Ci nmol^{-1}; see http://www.iem-inc.com/toolspa.html), less than microgram amounts of ^{57}Co in a sample may well be sufficient for measurements to obtain a good emission spectrum.

It has to be mentioned that through the 1960s, there was some concern about the possibility for the Mössbauer isotopes with parent nuclei that undergo electron capture or converted isomeric transition (i.e., which lead to high Auger ionization) to be useful for studying matter [6,8]. This was due to some studies that reported disruption of some Mössbauer isotope-containing molecules induced by the Auger ionization process [6]. As witnessed by

Mössbauer Spectroscopy: Applications in Chemistry, Biology, and Nanotechnology, First Edition.
Edited by Virender K. Sharma, Gostar Klingelhofer, and Tetsuaki Nishida.

Professor Amar Nath [6], Nobel Prize winner Willard F. Libby's comment on that point was, "What can you learn about a crystal vase using a sledge hammer?" Fortunately, this skepticism was not corroborated, as there are ways for the enormous energy (e.g., ~6 keV on the ^{57}Fe nuclei after ^{57}Co decay), formed on the daughter atom after nuclear transformation, to be dissipated in a solid [8,11]. However, owing largely to the specific methodological difficulties of this sophisticated nuclear chemistry technique (particularly the necessity of using a radioactive isotope in samples under study), the total number of yearly EMS-related publications have tended to decline from a maximum of about a hundred papers per year (reached in the 1970s) down to ca. 20 papers appearing annually by the 21st century [12].

Cobalt as a microelement has a number of biochemical and physiological functions in various organisms (see, for example, Ref. 5 and references reported therein). Despite its evident importance in biology and biomedicine-related fields and the unique sensitivity of ^{57}Co EMS, applications of this powerful technique in life sciences have so far been featured by a limited number of reports. Several reports on vibration characteristics of the ^{57}Co-labeled eardrum, basilar membrane and cochlea of the inner ear, and the hammer of the middle ear of various mammals were published within about a decade after 1964 (see Ref. 13, pp. 384–386). Those experiments were based on the sensitivity of the Mössbauer resonant system to Ångstrom-range vibration amplitudes [14,15]. While in those earlier studies ^{57}Co was used merely as an external physical EMS-active label, some contemporary and subsequent ^{57}Co EMS investigations involved intrinsically biology-related cobalt-containing complexes, for example, ^{57}Co-labeled cobalamins (vitamin B_{12} and its analogs) [16–18], porphyrins [16,17], and phthalocyanines [16,17,19]; hemoglobins [20,21] and other heme complexes [22]; and $^{57}Co^{II}$ complexes with various nucleotides [23–25]. In Ref. 26, the molecular dynamics in the ^{57}Co-doped protein concanavalin A was studied using ^{57}Co EMS.

Note that the experiments with the system ^{57}Co-labeled vitamin B_{12} coenzyme + the enzyme ethanolamine-ammonia lyase [17] represented the very first attempt to apply ^{57}Co EMS to an enzyme-related system, although in that case solely the coenzyme (B_{12}) was labeled with ^{57}Co. Unfortunately, all the emission spectra and the Mössbauer parameters calculated therefrom for the initial ^{57}Co-labeled coenzyme B_{12} and for the system [labeled coenzyme + enzyme] at various time points, up to the completion of the enzymic reaction, appeared to be virtually the same [17]. (It is important to emphasize that a successful enzymic assay of the sample [^{57}Co]-coenzyme + enzyme after Mössbauer measurements [17] proved that any radiation damage that might have taken place was not sufficient to affect significantly the biological activity of the system.) The conclusion made in Ref. 17, stating that "it is unlikely that ^{57}Co emission Mössbauer spectroscopy will contribute greatly to the understanding of vitamin B_{12}-dependent enzymes," although related exclusively to that system, seems to have damped down the enthusiasm of other researchers, who could be interested in applying EMS to enzyme-related systems. Nevertheless, already our first ^{57}Co EMS experiments involving a ^{57}Co-doped enzyme, bacterial glutamine synthetase (GS) [27] (to be discussed in more detail below), where an enzyme with ^{57}Co-doped active centers was for the first time studied using ^{57}Co EMS, appeared to be successful and gave a new stimulus for further related investigations.

Besides that, ^{57}Co EMS was earlier applied for monitoring the state of cobalt(II) in roots of water hyacinth *Eichhornia crassipes* [28], as well as in cells of a cyanobacterium (the blue-green alga *Synechococcus vulcanus*) [29] and Gram-negative bacteria (*Escherichia coli* [30] and, more recently, *Azospirillum brasilense* in the freeze-dried state [27,32] or in frozen aqueous suspensions (FAS) [31,32] after their contact with $^{57}Co^{II}$ in solution).

In this chapter, recent progress is reviewed considering the applications of the ^{57}Co EMS technique for studying ^{57}Co-doped enzyme samples as well as $^{57}Co^{II}$ binding and transformations in bacterial cells. Further developments, potentials, and future prospects of the ^{57}Co EMS methodology are also briefly discussed with the aim to broaden the scope of possible applications of this fascinating technique, which has so far remained uncommon in biochemistry, microbiology, and related biological fields.

17.2 METHODOLOGY

For the ^{57}Co radionuclide, the half-life period is 270 days. Its nuclear decay proceeding via electron capture gives the stable ^{57}Fe isotope and is accompanied by specific physical and chemical aftereffects (various details, consequences, and possible applications of ^{57}Co radioactive decay aftereffects with regard to ^{57}Co EMS measurements have been recently discussed, for example, in Refs. 5,6,8,10,11,33–36). The resulting recoil energy (ca. 4.6 eV) for the daughter ^{57}Fe nucleus is sufficiently low, so that the nucleogenic iron atoms do not shift from their positions, and in many cases their chemical state and environment reflect that of the parent ^{57}Co species.

However, as a result of the concatenated processes of consecutively filling in the vacancies in inner electronic shells of the ^{57}Fe atom after the electron capture by the ^{57}Co nucleus (the so-called Auger cascade developing within 10^{-15} to 10^{-14} s), Auger electrons are ejected out of the ^{57}Fe atom, giving a series of its different, mainly short-lived charge states. By the moment when a 14.4-keV γ-quantum is emitted by the nucleus (ca. 10^{-7} s after the electron capture), most of the Auger electrons return, giving common charge states of the daughter ^{57}Fe ions. Some of these charge states correspond to those of the parent ^{57}Co; however, the interaction of some Auger electrons with the chemical environment of the atom can result in the formation of (an)other charge state(s) of the latter. For example, for parent $^{57}Co^{II}$ species, along with the corresponding daughter $^{57}Fe^{II}$ species, some portion of $^{57}Fe^{III}$ species can be formed.

These aftereffects, which inevitably complicate the emission spectra, yet can provide valuable additional information, for example, on the electron-acceptor properties of the proximal coordination environment around ^{57}Co [37,38]. For instance, the higher the electron-acceptor properties of the microenvironment of the nucleogenic ^{57}Fe atom formed upon decay of $^{57}Co^{II}$, the higher the yield of the aliovalent $^{57}Fe^{III}$ form. Nevertheless, by the moment of emission of a 14.4 keV γ-quantum, commonly a major or substantial part of the resulting ^{57}Fe ions regain the charge of the parent ^{57}Co ion, staying essentially in the same coordination microenvironment. Thus, the resulting substance under EMS study may be regarded as a ^{57}Fe complex in which the nucleogenic ^{57}Fe ion substitutes for the parent ^{57}Co ion (retaining both its charge and largely the geometry of the surrounding donor atoms of the ligands).

As already mentioned, the recoil-free emission (as well as absorption) of γ-quanta (the Mössbauer effect) is observed in solids only; therefore, samples of solutions or liquids are usually studied in the rapidly frozen state [3]. Rapid freezing often allows crystallization of the liquid (solvent) to be avoided, so that the structure of the resulting glassy solid matrix represents that of the initial solution. Upon freezing, any chemical reactions in the system as well as biochemical (metabolic) processes in live cells, tissues, or other biological samples cease at a certain point. Thus, freezing a biological system under study after different periods of time allows time-dependent metabolic transformations to be monitored [5,30–32]. On the other hand, in cells or tissues kept above the freezing point, any noticeable Mössbauer effect can be detected only for ^{57}Co species that remain within (or at the surface of) quasisolid parts (e.g., cell membranes) or in a very viscous medium [30].

A typical conventional experimental setup for measuring emission Mössbauer spectra is schematically shown in Fig. 17.1 [5]. The ^{57}Co-containing sample (which in EMS is the source of γ-radiation) can be kept in a cryostat (e.g., in liquid nitrogen at $T \approx 80$ K), whereas the absorber vibrates along the axis "source–absorber" at a constant-acceleration value (with its sign periodically changing from $+a$ to $-a$) with a strictly defined time dependence of velocities (usually up to ± 10 mm s^{-1} relative to the sample), thus modifying the γ-quanta energy scale according to the Doppler effect.

Emission Mössbauer spectra are measured by placing a ^{57}Co-containing sample (as a source of γ-radiation) in a sample holder of the spectrometer (if necessary, it may be kept in a specially designed cryostat with a window for γ-rays) using a conventional constant-acceleration Mössbauer spectrometer combined with a PC-operated multichannel analyzer. The spectrometer is calibrated using a standard (e.g., α-Fe foil). In order to obtain suitable statistics, each spectrum is collected for some period of time, usually from a few hours up to several days, depending on the content of ^{57}Co in the sample and the Mössbauer effect [8,9]. Standard PC-based statistical analysis involves fitting the experimental data obtained (for EMS they are commonly converted into a form compatible with that of conventional absorption ^{57}Fe Mössbauer measurements, that is, with isomer shift values for the nucleogenic $^{57}Fe^{II}$ or $^{57}Fe^{III}$ positive with regard to α-Fe) as a sum of Lorentzian-shaped lines using a least squares minimization procedure. The usual set of Mössbauer parameters is thus calculated from the experimental data (all isomer shift (δ) values discussed in this chapter will be given relative to α-Fe at room temperature).

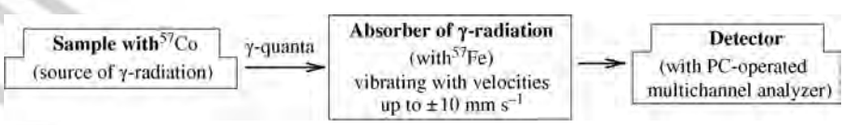

FIGURE 17.1

Scheme of experimental setup for measuring ^{57}Co emission Mössbauer spectra.

17.3 MICROBIOLOGICAL APPLICATIONS

Cobalt, being required as a trace element for both eukaryotes and prokaryotes, yet can induce toxic effects at higher concentrations (see Refs 5,27,39 and references therein). In particular, when present in the medium, Co^{II} (as well as some other heavy metals) is rapidly accumulated in most bacterial cells by the fast and unspecific membrane-integral protein CorA belonging to the metal-inorganic-transport (MIT) family. In many microorganisms, cobalt(II) is involved in diverse enzymatic activities [5,27] and can be included in intracellular magnetosomes [5]. However, its primary binding to the cell surface in the course of purely chemical and virtually nonselective processes can take place in both live and dead microbial cells [5,27]. Cobalt attracts attention also owing to biogeochemical problems resulting from the microbially mediated migration of the radionuclide ^{60}Co from disposal sites [27,31]. Such processes can be facilitated by release of cobalt traces entrapped within ferric oxide minerals upon the microbial dissimilatory reduction of iron(III) [22] together with possible Co^{3+} species [31]. In view of the aforementioned, knowledge of microbiological transformations of cobalt is of importance both from the analytical viewpoint and for its chemical speciation.

Virtually the first report on ^{57}Co EMS measurements in bacteria concerned the accumulation of $^{57}Co^{2+}$ complex with a bacterial hexadentate iron(III)-chelating agent, enterochelin (a cyclic trimer of *N*-2,3-dihydroxybenzoylserine) in cells of *E. coli* (strain AN 272) [30]. Measurements were performed both for frozen bacterial samples (at $T = 83$ K) and above the freezing point (at $+3\,^{\circ}$C). Interestingly, in the latter case a very weak but distinguishable effect ($\sim$0.03%, with a width about 3 mm s^{-1}) was detected for 24 h, after which no effect was any longer observed. Disappearance of the effect was ascribed [30] to damage that might have occurred to the cells under the experimental conditions applied. For frozen bacteria, the effect was much higher and resulted in accumulating relatively good spectra within 4 days (no Mössbauer parameters were reported). By comparing the data obtained, it was assumed that about 4% of the $^{57}Co^{2+}$ complex absorbed by the bacteria were located within the cell membrane (a quasisolid cellular structure), thus giving some weak but noticeable effect without freezing.

A similar EMS study was performed on ^{57}Co in thermophilic cyanobacteria (blue-green alga, *Synechococcus vulcanus*) incubated with carrier-free $^{57}Co^{2+}$ salt for 4 months at 55 °C [29]. The cell suspension was centrifuged, and live cells were rinsed with ^{57}Co-free nutrient solution and frozen in liquid nitrogen, as *in vivo* measurements gave no appreciable effect. The data obtained were compared with absorption (^{57}Fe) Mössbauer measurements on iron species in cells of the alga (cultivated for up to 6 days with $^{57}Fe^{III}$–EDTA complex), which were totally different. The most appropriate fit of the emission spectrum presented in Ref. 29, comprising a superposition of two quadrupole-split components, yielded a major doublet (74% of the total spectral area) with the parameters (isomer shift $\delta = 0.27 \pm 0.01$ mm s^{-1}, quadrupole splitting $\Delta E_Q = 2.08 \pm 0.01$ mm s^{-1} at liquid nitrogen temperature) similar to those of ^{57}Co-doped cobalamins [16] and related complexes. The minor quadrupole doublet (26% of the total spectral area; $\delta = 1.08 \pm 0.01$ mm s^{-1}, $\Delta E_Q = 2.66 \pm 0.01$ mm s^{-1}) was ascribed to a high-spin ferrous species not found in other ^{57}Co cobalamins. This component was assumed to be a result of biological reactions involving ^{57}Co in cyanobacterium cells.

Note for comparison that the emission spectrum of the $^{57}Co^{II}$-doped cyanobacteria was found to be different from that of ^{57}Co in roots of water hyacinth [28]. The Mössbauer parameters for frozen roots of water hyacinth that had been cultivated for 2 weeks with $^{57}Co^{II}$ salt (a quadrupole doublet of high-spin ferrous component with $\delta = 1.19 \pm 0.05$ mm s^{-1}, $\Delta E_Q = 2.66 \pm 0.05$ mm s^{-1}, 56% of the total spectral area, and an accompanying doublet with $\delta = 0.45 \pm 0.1$ mm s^{-1}; $\Delta E_Q = 1.6 \pm 0.1$ mm s^{-1}, 44% of the total spectral area, as a result of aftereffects) indicated that cobalt is possibly complexed with an EDTA chelating agent from a nutrient solution or another chelating compound of plant origin. Indeed, the Mössbauer parameters for $^{57}Co^{II}$–EDTA complex at pH 6.6 in frozen solution ($\delta = 1.17 \pm 0.05$ mm s^{-1}, $\Delta E_Q = 2.71 \pm 0.05$ mm s^{-1}, 80% of the total spectral area, and an accompanying doublet with $\delta = 0.6 \pm 0.1$ mm s^{-1}, $\Delta E_Q = 1.6 \pm 0.1$ mm s^{-1}, 20% of the total spectral area, as a result of aftereffects) [28] are very similar, except for the yield of the aliovalent ferric component (as a result of aftereffects). In its turn, the parameters of the latter are very close to those calculated from the absorption spectrum of the $^{57}Fe^{III}$–EDTA complex in frozen solution at pH 4 ($\delta = 0.46 \pm 0.03$ mm s^{-1}, $\Delta E_Q = 1.64 \pm 0.03$ mm s^{-1}).

In the soil diazotrophic rhizobacterium *A. brasilense* (strain Sp245, reported to be tolerant to submillimolar concentrations of heavy metals, including cobalt(II), in the culture medium [32]), EMS studies were first performed on freeze-dried bacterial samples (measured at $T = 80$ K; Fig. 17.2) [27]. The following experiments with the same bacteria were performed with live cells rapidly frozen after certain periods of time (2–60 min) of contact with $^{57}Co^{II}$, and EMS spectra were measured for frozen suspensions (without drying), which more closely represent the state of cobalt in the live cells [31,32] (Fig. 17.3) . Mössbauer parameters calculated from the experimental data are listed in Table 17.1.

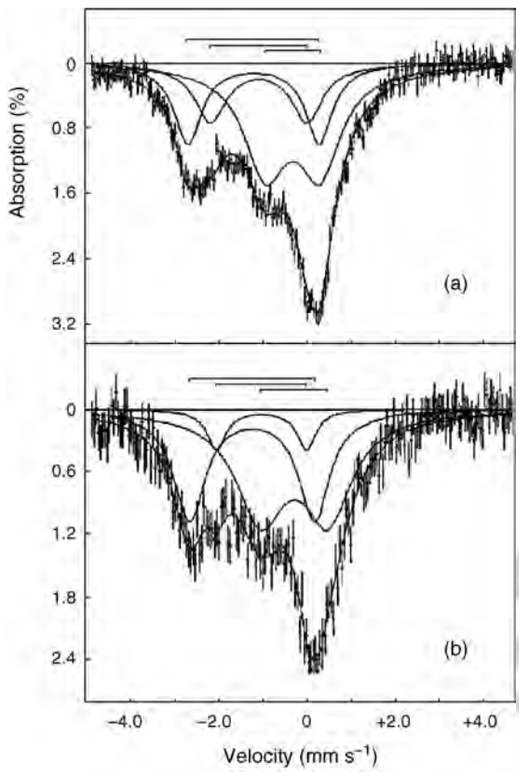

FIGURE 17.2

Emission Mössbauer spectra of dried cells of *Azospirillum brasilense* (strain Sp245) that were incubated as live cells with $^{57}CoCl_2$ for 2 min (a) and 60 min (b) at ambient temperature, then rapidly frozen in liquid nitrogen and freeze-dried prior to EMS measurements (spectra measured at $T = 80$ K; see also Table 17.1). The positions of spectral components (quadrupole doublets) composing the whole spectrum (solid envelope), obtained by fitting the experimental data (points), are shown above the spectra with square brackets; the same for other figures with emission spectra. (Adapted from Ref. 27.)

For each of the aforementioned cell samples, there were two EMS components corresponding to two chemical forms of high-spin $^{57}Co^{II}$. (The presence of the third component with the parameters typical for high-spin nucleogenic iron(III), stabilized after nuclear decay of the parent $^{57}Co^{2+}$ ion, is evidently a result of aftereffects of the $^{57}Co \rightarrow {}^{57}Fe$ nuclear transformation, as Co^{III} is not expected to appear in such systems.) The presence of at least two major cobaltous forms (with different δ and ΔE_Q values, see Table 17.1) revealed in the spectra of cells may be related to the availability of different functional groups (also with possibly different donor atoms) as ligands at the bacterial cell surface (see, for example, Refs 31,32 and references therein).

It is noteworthy that the main parameters (δ, ΔE_Q, and even Γ) of the corresponding (+2)-forms for live bacterial cells measured in the dry state and in frozen aqueous suspension were found to be statistically indistinguishable or very close both for 2 min (see Table 17.1, sample 1; cf. frozen aqueous suspension (FAS) and dried biomass (DB)) and for 1 h of contact with $^{57}Co^{2+}$ (sample 2; cf. FAS and DB). This finding shows that freeze-drying does not significantly affect the chemical state of the cobalt(II) species bound at the surface or within the membrane of the bacterium, once their parameters remain virtually unchanged. There was some redistribution of the relative contents of the forms (featured by the corresponding *S* values; see Table 17.1) in going from the hydrated (FAS) state to the dry (DB) state (samples 1 and 2; note, in particular, the increased *S* values for $^{57}Fe^{3+}$ in the DB state). This might be related to the changes in the yield of the (+3) form (resulting from aftereffects) in going from the aqueous medium to the dry biomass (e.g., due to possible changes in the outer coordination sphere of $^{57}Co^{2+}$ complexes occurring upon removal of excess water). Another contribution to this effect could partly be made by nonequal changes in the recoilless emission probability (Mössbauer–Lamb factor) for different forms upon drying.

In Fig. 17.4, the Mössbauer parameters are plotted for different cobalt(II) forms in each sample and for various periods of contact (2 and 60 min) of the live bacteria with $^{57}Co^{II}$, as well as for dead bacterial cells (thermally killed by storing in the medium at 95 °C in a water bath) and for the cell-free supernatant liquid [5,31]. The EMS data for different periods (2 min and 1 h) of contact of live bacteria with $^{57}Co^{2+}$ traces essentially differed in the corresponding QS values (see Table 17.1) for the two (+2) forms [31]. This finding indicated that within an hour, after primary rapid adsorption onto the cell surface, cobalt(II) underwent further transformation, most probably occurring within the cell membrane. Nevertheless, the parameters for live bacteria after 2 min and for dead bacteria were found to be rather close (essentially

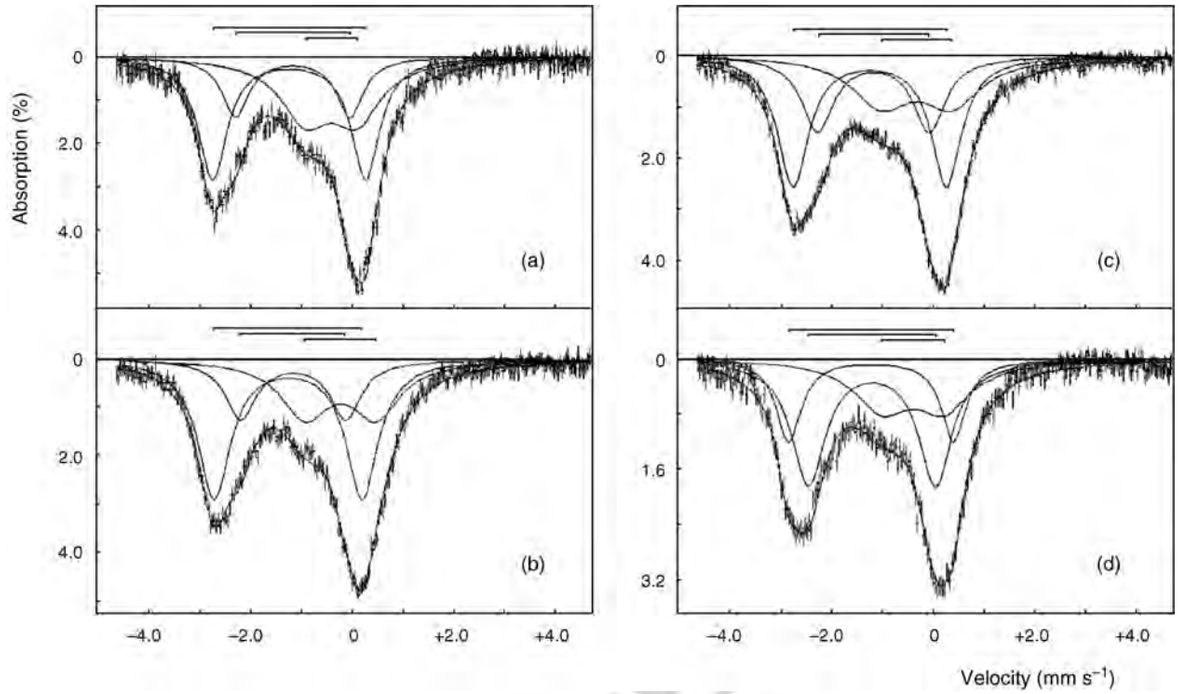

FIGURE 17.3

Emission Mössbauer spectra of frozen aqueous suspensions of live (a, b) and dead (c) cells of *Azospirillum brasilense* (strain Sp245) in the culture medium as well as of the cell-free supernatant liquid (d), that were incubated with $^{57}CoCl_2$ for 2 min (a) and 60 min (b–d) at ambient temperature and then rapidly frozen in liquid nitrogen (spectra collected at $T = 80$ K; see also Table 17.1). (Adapted from Ref. 32.)

overlapping). This finding indicates that the mechanism of primary rapid Co^{2+} sorption by live cells of this strain is similar to the purely chemical binding process occurring at the surface of dead (thermally killed) cells, and is virtually not affected by such hydrothermal treatment. Some differences in the parameters for the stabilized (+3)-form, resulting from aftereffects, for samples 1 (FAS) and 3 in Table 17.1, and its lower content in sample 3 might be related to some possible changes in the properties of cell-surface biopolymers induced by the hydrothermal treatment.

Neither of the (+2) components found in all of the samples, including cell-free supernatant liquid, corresponded to the aquo complex $[^{57}Co(H_2O)_6]^{2+}$, as the latter is featured by IS = 1.3–1.4 mm s^{-1} and QS = 3.3–3.4 mm s^{-1} in frozen aqueous solutions (see, for example, Ref. 3, Chapters 4 and 5). Note also that the parameters for the cell-free supernatant liquid (from which the bacterial cells had been removed by centrifugation) were clearly different from those for all the other samples (see Fig. 17.4). Thus, in the cell-free supernatant liquid the chemical state of Co^{2+} trace species (i.e., Co^{2+} complexes) was different from those in cell samples. In its turn, this shows that in the presence of bacterial cells, Co^{2+} traces are completely (and, considering sample 1, also rapidly, within 2 min) bound by the cells.

In the cell-free culture solution, the most likely ligands that could bind Co^{2+} are phosphate and possibly malate anions (present in the initial standard growth medium at concentrations of the order of 10^{-2} M), ammonia (from NH_4^+ added to the initial medium at ~5 mM), as well as various (probably acidic) exopolysaccharides dissolving from the cell surface [31,32]. Note that both malate and NH_4^+ are gradually consumed by the growing bacteria as sources of carbon and bound nitrogen. Thus, the majority of donor atoms in the first coordination spheres of $^{57}Co^{2+}$ complexes in the cell-free solution are likely to be represented by oxygen (including that of hydration water molecules) and probably nitrogen.

It has to be admitted that direct identification of metal complexes in such sophisticated systems as bacterial cells using ^{57}Co EMS is so far difficult for several reasons. First, there is still lack of experimental EMS data on model cobalt biocomplexes [41], which could facilitate interpretation of EMS parameters. Second, various chemical species with structurally (with regard to the coordination symmetry and arrangement of donor atoms around the cation) and compositionally (with regard to the nature of donor atoms of the ligands) similar coordination microenvironments can give similar Mössbauer parameters. Also, in EMS, the Auger electrons formed during the Auger cascade inevitably

TABLE 17.1 Mössbauer Parameters[a] Calculated from Emission Mössbauer Spectroscopic Data for Aqueous Suspensions of Live and Dead Cells of *Azospirillumbrasilense* Sp245 in the $^{57}Co^{II}$-Containing Culture Medium as well as for the Cell-Free Supernatant Liquid, which were Incubated with $^{57}CoCl_2$ for Specified Periods of Time at Ambient Temperature and then Rapidly Frozen in Liquid Nitrogen (Spectra Measured at $T = 80$ K) [27,31,32])

Sample	State[b]	Oxidation State[c]	δ [d] (mm s^{-1})	ΔE_Q [e] (mm s^{-1})	Γ[f] (mm s^{-1})	S [g] (%)
1. Live bacterial cells (frozen 2 min after adding $^{57}CoCl_2$ to the culture medium)	FAS	+2	1.26(1)	3.00(3)	0.69(3)	44
		+2	1.20(6)	2.23(6)	0.65(8)	20
		+3	0.45(5)	1.0(1)	1.2(1)	36
	DB	+2	1.24(3)	3.08(6)	0.70(10)	19
		+2	1.14(3)	2.35(9)	0.83(13)	23
		+3	0.35(5)	1.26(8)	1.43(12)	58
2. Live bacterial cells (frozen 60 min after adding $^{57}CoCl_2$ to the culture medium)	FAS	+2	1.26(1)	2.89(2)	0.78(2)	51
		+2	1.16(1)	2.03(4)	0.73(6)	20
		+3	0.24(2)	1.40(3)	1.13(6)	29
	DB	+2	1.22(4)	2.84(7)	0.88(10)	38
		+2	1.00(5)	2.03(9)	0.5(2)	8
		+3	0.26(5)	1.55(7)	1.36(16)	54
3. Dead bacterial cells (frozen 60 min after adding $^{57}CoCl_2$)	FAS	+2	1.24(1)	3.00(2)	0.73(2)	44
		+2	1.17(1)	2.18(4)	0.76(4)	27
		+3	0.33(3)	1.39(6)	1.4(1)	29
4. Supernatant liquid (frozen 60 min after adding $^{57}CoCl_2$)	FAS	+2	1.22(1)	3.23(5)	0.60(2)	24
		+2	1.21(1)	2.48(3)	0.80(3)	48
		+3	0.40(6)	1.22(3)	1.3(2)	28

[a]Errors (in the last digits) are given in parentheses.
[b]FAS, frozen aqueous suspension (or frozen aqueous solution in case of sample 4); DB, dried biomass.
[c]Oxidation states of the nucleogenic ^{57}Fe components stabilized after nuclear decay of the parent $^{57}Co^{II}$.
[d]Isomer shift (relative to α-Fe) converted to the normal absorption convention.
[e]Quadrupole splitting.
[f]Full line width at half maximum (assumed to be equal for both lines of a doublet).
[g]Relative resonant absorption areas (relative error $\pm$4%) of the relevant spectral components.

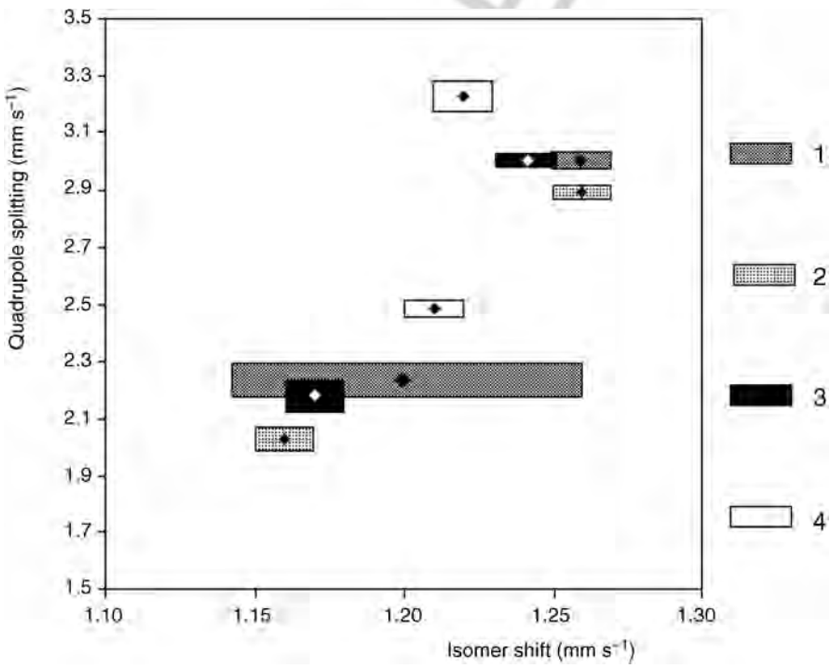

FIGURE 17.4
Mössbauer parameters—isomer shift (δ, mm s^{-1}; relative to α-Fe) and quadrupole splitting (ΔE_Q, mm s^{-1})—plotted for different forms of $^{57}Co^{II}$ in aqueous suspension of live cells of *Azospirillum brasilense* (strain Sp245) rapidly frozen after (1) 2 min and (2) 60 min of contact with $^{57}Co^{II}$, (3) dead cells (hydrothermally killed at 95 °C), and (4) cell-free supernatant liquid (measured at $T = 80$ K). (Adapted from Ref. 5.)

TABLE 17.2 Mössbauer Parameters Calculated from ^{57}Co Emission Spectroscopic Data for Live or Dead Cells of *A. brasilense* (strain Sp7) Incubated with $^{57}CoCl_2$ for 2 min or 1 h and then Rapidly Frozen in Liquid Nitrogen (Measured at $T = 80$ K), in Frozen Aqueous Suspension (s) or Dried (d) [40]

Bacterial Cells	Multiplet[a]	δ [b] (mm s^{-1})	ΔE_Q [c] (mm s^{-1})	S [d] (%)
Live (2 min), s	Doublet 1	1.10	2.59	56
	Doublet 2	0.89	2.00	19
Live (1 h), s	Doublet 1	1.16	2.84	35
	Doublet 2	1.02	2.18	31
Dead (1 h), s	Doublet 1	1.17	2.75	45
	Doublet 2	1.00	2.13	28
Live (2 min), d	Doublet 1	1.18	2.79	55
	Doublet 2	1.12	1.84	10
Live (1 h), d	Doublet 1	1.14	2.93	43
	Doublet 2	1.07	2.25	23
Dead (1 h), d	Doublet 1	1.17	2.78	57
	Doublet 2	1.04	1.95	7

Errors: for δ, ± 0.02 mm s^{-1}; for ΔE_Q, ± 0.05 mm s^{-1}; for S, ± 7 rel.%.
[a]Main doublets corresponding to daughter Fe^{II} forms stabilized after the $^{57}Co \rightarrow {}^{57}Fe$ nuclear transition (the residual Fe^{III} forms result from aftereffects).
[b]Isomer shift (relative to α-Fe at room temperature).
[c]Quadrupole splitting.
[d]Relative resonant absorption area.

influence to some extent the coordination environment of the nuclide, even if its chemical state remains unchanged, which, in particular, results in some noticeable line broadening in ^{57}Co emission spectra (as compared to absorption spectra of the corresponding ^{57}Fe compounds) [33–35].

Recently, comparative ^{57}Co EMS studies at $T = 80$ K were carried out also for live and dead (hydrothermally treated) cells of another *A. brasilense* strain, Sp7, in frozen aqueous suspensions and as dried residues (in Table 17.2, the parameters of the main (+2)-components are listed) [40]. Note that this bacterium represents a good model for studying its responses to ecological factors. Its strain Sp245 (see above) is an endophyte (capable of penetrating into and colonizing the plant root tissues), whereas strain Sp7 is an epiphyte (colonizing the root surface only). Thus, the two strains occupy different ecological niches and can show marked differences in behavior under similar conditions [32]. Live cells of strain Sp7 rapidly frozen 2 min and 1 h after their contact with $^{57}Co^{2+}$ (measured in frozen suspensions) also showed marked differences in their Mössbauer parameters, similarly reflecting metabolic transformations of $^{57}Co^{2+}$ occurring within an hour. However, the parameters for strains Sp245 [31] and Sp7 [40] (see Tables 17.1 and 17.2), obtained under similar conditions, also differ, implying dissimilarities in their metabolic responses to Co^{2+} detected earlier using FTIR spectroscopy [32].

17.4 ENZYMOLOGICAL APPLICATIONS

17.4.1 Choosing a Test Object

The ^{57}Co EMS technique has recently been shown for the first time to be applicable to probing cation-binding sites of the enzyme active centers [27]. As the first example of a metal-dependent enzyme tested with ^{57}Co EMS [27,42], a bacterial glutamine synthetase (GS, EC 6.3.1.2; a key enzyme of nitrogen metabolism that is ubiquitous in all organisms from bacteria to humans) was used. For instance, in humans, GS is expressed in tissues, being involved in ammonia detoxification and interorgan nitrogen flux; its malfunctioning or inherited deficiency was found to lead to multiple disorders of organs and brain malformation [43]. There were logical reasons for choosing this particular enzyme, isolated from the soil diazotrophic bacterium *A. brasilense*, for testing the validity of data obtained by the EMS technique. A few main reasons are considered below.

First, cobalt(II) is among its activating divalent cations (cofactors), along with Mg^{2+} and Mn^{2+} [44]. It was found that the enzyme could be obtained in a cation-free state (by removing the native cation(s) bound in the active centres using EDTA treatment with subsequent dialysis), in which it loses its biocatalytic activity in the absence of divalent cations in the

medium. By adding Co^{2+} to the inactive metal-free GS it was possible to reinstate its activity, thereby proving that the added Co^{2+} cations bind in the active centres (the latter is prerequisite for the GS activity to be expressed) [44,45]. Thus, doping the cation-free GS with a precalculated amount of $^{57}Co^{2+}$ under physiologically similar conditions in principle allows ^{57}Co EMS to be applied.

Second, this enzyme has *two* cation-binding sites (n1 and n2) at each of its 12 active centers (i.e., total 24 sites) per molecule [44]. From the structural point of view, a molecule of bacterial GS is a dodecamer formed from two hexameric rings of subunits (monomers) disposed face-to-face (Fig. 17.5a); each of the 12 active centers (having the shape of a 'bifunnel'; Fig. 17.5b) is located between every two neighboring subunits within a ring. Site n1 has ca. 50-fold greater affinity for cations than site n2, which is related to their coordination modes and charge distribution [42]. In site n1, the cation is coordinated by three glutamic acid (Glu) residues (E131, E212, and E220), that is, by their three side-chain carboxylates (with possible additional binding of H_2O), while in site n2 by two Glu (E129 and E357) and one histidine, H269 (i.e., one N-donor atom of the His heterocycle and two Glu carboxyls), and this structure is strictly conserved among different GSs [43].

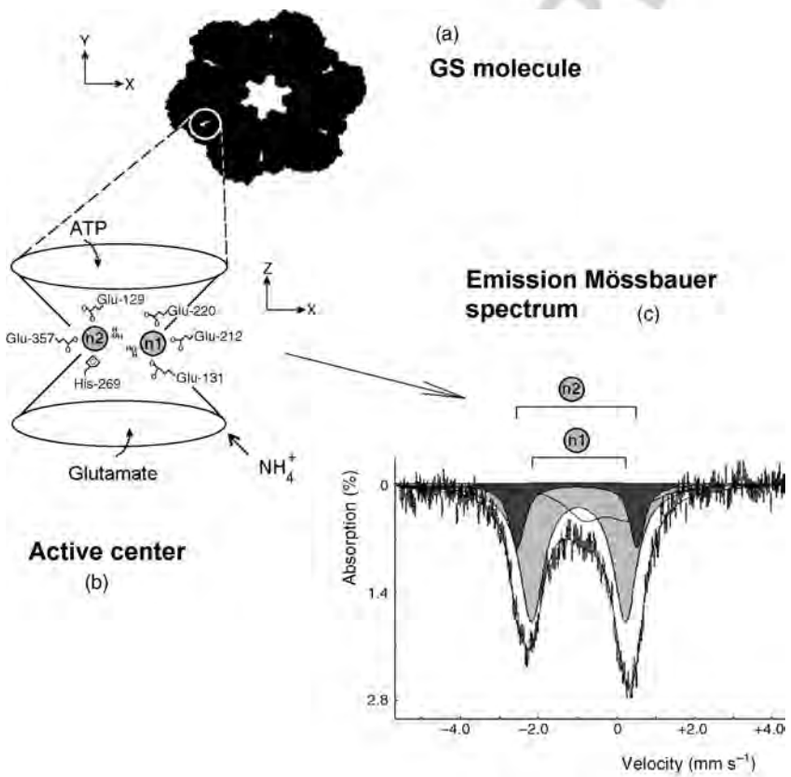

FIGURE 17.5

Schematic presentation of (a) a top view of one of the two hexameric rings of a bacterial glutamine synthetase molecule (the position of an active center in an intersubunit space is shown by white circle); (b) a side-view of the active center ('bifunnel', ca. 1.5 nm wide and 4.5 nm high, with metal ions in two cation-binding sites, n1 and n2), which ATP and glutamate enter at opposite ends as shown; and (c) an emission Mössbauer spectrum of cation-free GS from *Azospirillum brasilense* (in an average adenylylation state of 18%) doped with $^{57}Co^{2+}$ (measured in rapidly frozen aqueous solution; $T = 80$ K) [42]. The subspectra featuring sites n1 (light-shaded doublet) and n2 (dark-shaded doublet) are indicated by accordingly marked square brackets above the spectrum (the third broader doublet of lower intensity is due to aftereffects of the $^{57}Co \rightarrow {}^{57}Fe$ nuclear transformation [27]). Relative resonant absorption of γ-quanta (in percent) by a standard absorber ($K_4Fe(CN)_6 \cdot 3H_2O$) is plotted against relative velocity of the absorber versus the ^{57}Co-containing sample (γ-radiation source) [8], which corresponds to the energy scale according to the Doppler effect (± 1 mm s^{-1} corresponds to ± 48.1 neV), calibrated using α-Fe at room temperature. (Adapted from Ref. 43.)

The cations in these two sites are 0.6 nm apart, have no common ligands (i.e., not bridged) and therefore, from the spectroscopic point of view, may be regarded as relatively independent from each other. Thus, sites n1 and n2, when both occupied by $^{57}Co^{2+}$ cations, could be expected to exhibit different Mössbauer parameters in an emission spectrum (i.e., giving distinguishable spectral components) owing to their essentially different coordination microenvironments. Moreover, since the affinity for cations is much higher in site n1, in case when the molar $^{57}Co^{2+}$-to-GS ratio (x) is made higher than that required to saturate half of all the sites (i.e., primarily sites n1) but under the 'saturation limit' for both n1 + n2 (i.e., under the condition $12 < x < 24$), the resulting ratio of the areas for the subspectra (spectral components) corresponding to n1 and n2 could be expected to allow $^{57}Co^{2+}$ distribution between the sites to be assessed (Fig. 17.5c) [45].

17.4.2 Prerequisites for Using the ^{57}Co EMS Technique

In order for the enzyme, with its active centers doped with $^{57}Co^{2+}$, to be useful in EMS, a correct analysis of the EMS data to be obtained is necessary. Thus, several conditions have to be observed [45].

First, it is important to make sure that the $^{57}Co^{2+}$ cations, substituting for the native metal(II) ions [44], are indeed bound within the active centers. If this is not so, the existence of numerous binding sites and, consequently, many forms of $^{57}Co^{II}$ bound to functional groups of the protein macromolecule would render the EMS data hardly interpretable.

Second, the replacement of the native activating cations (e.g., by natural Co^{2+} under identical conditions) ideally should not result in an irreversible deactivation of the enzyme. In the latter case, the correspondence between the $^{57}Co^{II}$ form in the enzyme sample under study and the cobalt(II) form in the physiologically active enzyme would be doubtful.

Finally, the quantity of the substituted $^{57}Co^{2+}$ should conform to the overall number of the cation-binding sites in the enzyme sample. Any excessive $^{57}Co^{2+}$, binding to different functional groups of the protein beyond the active centers, would evidently lead to an unpredictable complication of the spectra.

As the affinity for cations in the enzyme active centers is usually much higher than elsewhere on the protein globule, the above-mentioned conditions may well be feasible. Moreover, when the active center contains more than one cation-binding site with different affinities for the cation (but high, as compared to any other possible binding sites beyond active centers) and different coordination environments (as in the case with glutamine synthetase [43]), it may be expected that ^{57}Co EMS would allow one to obtain information not only on the chemical forms and coordination symmetry of the cobalt in each of the sites but also on its distribution between them. The above-discussed properties of *A. brasilense* GS were found to be suitable for using EMS in studying $^{57}Co^{2+}$-doped enzyme preparations [5,7,27,45].

17.4.3 Experimental ^{57}Co EMS Studies

Analysis of the emission Mössbauer spectra of [^{57}Co]-cobalt(II)-doped GS (in a low average adenylylation state, 18%) both in rapidly frozen aqueous solution [27] and in the solid state [42] indeed revealed the presence of two forms of cobalt(II) with different affinities (in view of nonequal distribution of $^{57}Co^{II}$ between the forms; Fig. 17.6) as well as with different coordination reflected by different Mössbauer parameters (Table 17.3) . However, each of the relevant forms in dissolved and solid enzyme showed similar (significantly overlapping) parameters. This is indicative of a close similarity of the cobalt(II) coordination structure in enzyme's active centers both in solution and in the dry state, which reflects the well-known fact of stability of the enzyme upon drying.

The values of isomer shifts ($\delta = 1.08$ and 1.05–1.07 mm s^{-1} relative to α-Fe) and quadrupole splittings ($\Delta E_Q =$ 3.0–3.1 and 2.3–2.4 mm s^{-1}; see Table 17.3) obtained for the two doublets allowed those components to be correlated with the two cation-binding sites in the GS active center (sites n2 and n1, respectively [42–44]). As mentioned above, these sites of bacterial GSs have different coordination environments, as well as a correspondingly lower (for site n2) and higher (for site n1) affinity to the cation. The latter difference is in line with the nonuniform distribution of $^{57}Co^{II}$ between the spectral components (as the areas of quadrupole doublets 1 and 2 in each spectrum corresponding to different $^{57}Co^{II}$ forms are significantly different; see Fig. 17.6).

It may be reasonably supposed that the nucleogenic $^{57}Fe^{II}$ form with a lower $\Delta E_Q = 2.3$–2.4 mm s^{-1} corresponds to the site with more symmetrically coordinated O-donor ligands, that is, site n1 (see Fig. 17.5b). In this case, the higher ΔE_Q value (ca. 3.0–3.1 mm s^{-1}) may reflect a lower coordination symmetry owing to different donor atoms including, along with oxygens, also the His-269 nitrogen (the δ values are close in these cases).

The relatively low IS values for both the $^{57}Co^{II}$ forms in GS with a low (18%) adenylylation state of its subunits (IS = 1.05 and 1.08 mm s^{-1} at $T = 80$ K; Table 17.3) may indicate a tetrahedral (T_d) symmetry of cobalt(II) coordination. In this case, the coordination mode of all the Glu residues must be monodentate, which is often observed for cation-binding

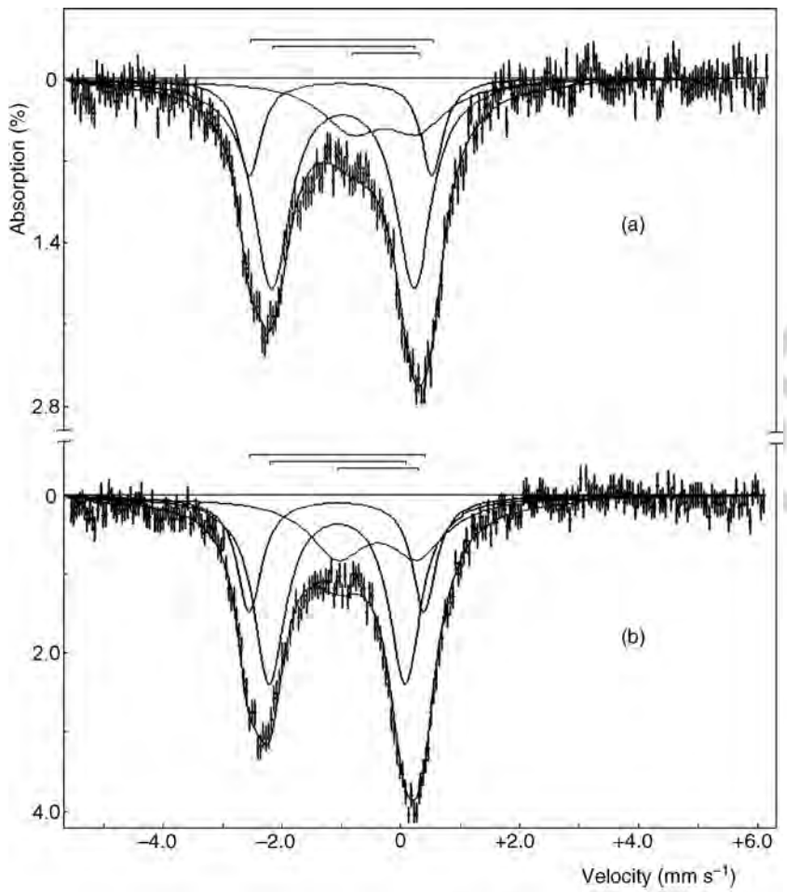

FIGURE 17.6

Emission Mössbauer spectra of cation-free glutamine synthetase (GS; average adenylylation state 18%) from *Azospirillum brasilense* Sp245 incubated with $^{57}Co^{2+}$ for 60 min at ambient temperature, measured (a) in rapidly frozen aqueous solution and (b) as a dried solid ($T = 80$ K; see also Table 17.3). (Adapted from Ref. 42.)

sites in metalloproteins (note that there is also at least one water molecule as a ligand) [43]. For comparison, the δ values reported for several high-spin carboxylate-rich Fe^{II} complexes (some with N-donor atoms, measured at $T = 4.2$ K) are within the range (1.04–1.08) $\pm$ 0.02 mm s^{-1} for the T_d geometry of the sites and (1.26–1.35) $\pm$ 0.02 mm s^{-1} for the octahedral (O_h) geometry [46]. Complexes of $^{57}Co^{II}$ with anthranilic (*o*-aminobenzoic) acid and L-tryptophan, studied using ^{57}Co EMS in frozen aqueous solutions, showed, respectively, $\delta = 1.10 \pm 0.02$ and 0.88 ± 0.06 mm s^{-1},

TABLE 17.3 Mössbauer Parameters[a] for $^{57}Co^{2+}$-Doped Glutamine Synthetase (GS, Average Adenylylation State 18%) from *Azospirillumbrasilense* Sp245 Calculated from Emission Mössbauer Spectra in Rapidly Frozen Aqueous Solution and in the Solid State (Measured at $T = 80$ K) [42]

Sample	O.S.[b]	δ [c] (mm s^{-1})	ΔE_Q [d] (mm s^{-1})	Γ[e] (mm s^{-1})	S[f] (%)
1. Cation-free GS incubated with $^{57}Co^{2+}$ for 60 min;	+2	1.08(0.02)	3.08(0.08)	0.48(0.05)	18(1)
frozen in liquid nitrogen (solution)	+2	1.05(0.02)	2.39(0.06)	0.75(0.08)	60(1)
	+3	0.34(0.10)	1.12(0.20)	1.25(0.30)	22(1)
2. Cation-free GS incubated with $^{57}Co^{2+}$ for 60 min,	+2	1.08(0.02)	2.97(0.06)	0.52(0.12)	24(1)
frozen and dried (solid)	+2	1.07(0.02)	2.29(0.06)	0.66(0.08)	50(1)
	+3	0.39(0.10)	1.37(0.20)	1.19(0.27)	26(1)

[a] Relative errors are given in parentheses.
[b] Oxidation state for the nucleogenic ^{57}Fe components stabilized after nuclear decay of the parent $^{57}Co^{II}$.
[c] Isomer shift (relative to α-Fe; converted to the normal absorption convention).
[d] Quadrupole splitting.
[e] Full linewidth at half maximum.
[f] Relative resonant absorption areas of the relevant spectral components.

$\Delta E_Q = 2.71 \pm 0.05$ and 2.8 ± 0.1 mm s^{-1} [41], which is also within the range for high-spin T_d coordination. Note that solid Fe^{II} anthranilate Fe(*anthr*)$_2$ with an O_h coordination (with two bidentate carboxylates and two amino groups as ligands, that is, 4O + 2N donor atoms) gave $\delta = 1.25 \pm 0.01$ mm s^{-1} (at $T = 80$ K) [41]. It may be expected that any intermediate coordination state of the activating cations, for example, occurring during substrate turnover in the course of the enzymatic reaction, could be distinguished using a rapid freeze-quench variant [2] applied to ^{57}Co EMS.

An extremely important issue for the ^{57}Co EMS methodology is the study of aftereffects of the $^{57}Co \rightarrow {}^{57}Fe$ radioactive decay process. For a complicated biocomplex, for example an enzyme, especially with more than one cation-binding site ($n > 1$) at the active center, each of the parent $^{57}Co^{II}$ chemical species (with its own coordination microenvironment) would, in principle, give its own yield of the aliovalent $^{57}Fe^{III}$ form (as a result of aftereffects). It is often the case when such daughter $^{57}Fe^{III}$ lines in the source experiment have very close parameters and, being also relatively broad, virtually do not resolve in the spectrum and thus have to be fitted with a single doublet. Since the partial yields for the *n* aliovalent $^{57}Fe^{III}$ forms remain unknown, the *real* distribution of $^{57}Co^{II}$ between the *n* sites in the sample under study is therefore also unknown, even when the corresponding *n* lines for $^{57}Fe^{II}$ do resolve and can easily be quantitatively assessed.

It has been shown that if a redistribution of $^{57}Co^{II}$ between *n* sites can be experimentally achieved, then solving a system of equations based on the material balance and using the data of *n* experimental ^{57}Co EMS measurements allow both the partial yields of $^{57}Fe^{III}$ (aftereffects) for each parent $^{57}Co^{II}$ form and the *real* distribution of $^{57}Co^{II}$ between the sites to be obtained [36]. This new methodology was applied to the aforementioned $^{57}Co^{II}$-doped bacterial glutamine synthetase (with $n = 2$ different cation-binding sites at its active centers). For that, the experimental data were used on the redistribution of $^{57}Co^{2+}$ between the sites found upon adding Mn^{2+} together with $^{57}Co^{2+}$ as a result of their competitive binding [47]. Moreover, it was of interest to compare the calculated yields of $^{57}Fe^{III}$ for the two enzyme sites (with coordinated carboxylic groups of three Glu amino acid residues and with two Glu + one His residues, respectively) with those for some $^{57}Co^{II}$–(aromatic amino acid) complexes in their emission spectra [41]. It was found that some functional groups—potential electron acceptors (aromatic cycles within the ligands coordinated to $^{57}Co^{II}$), located at various distances from parent $^{57}Co^{2+}$ ions (e.g., up to direct coordination via a N heteroatom), respectively, influence the yield of $^{57}Fe^{III}$ due to aftereffects. This is in line with a virtually large yield of aliovalent $^{57}Fe^{III}$ in emission spectra of $^{57}Co^{II}$–nucleotide complexes [23–25], in which the cation is directly bound to the N7 of the purine ring. Such studies facilitate understanding the appearance and regularities of aftereffects, which is necessary for adequately interpreting EMS data on sophisticated biocomplexes and for further successful biological and biochemical EMS applications.

17.4.4 Two-Metal-Ion Catalysis: Competitive Metal Binding at the Active Centers

Besides GS (both type I and type II), a number of other metal-dependent enzymes including, for example alkaline phosphatases, endonucleases, DNA/RNA polymerases, and so on, require two metal cations bound in the active center for their catalytic activity [43]. It has, however, to be noted that while, for instance, in polymerases and nucleases the two cations are coordinated *jointly* by both a conserved Asp residue and the scissile phosphate, in GS the two cations are bound by a few *separate* amino acid residues (see Fig. 17.5b). Moreover, the GS substrates bind to different cations (glutamate to n1 and ATP to n2; NH_4^+ has its separate binding site close to n1). This is in line with a relatively large distance between the two cations in GS (0.6 nm), as compared to those in, for example, RNases (0.4–0.3 nm) [43].

For *A. brasilense* GS, the possibility of the simultaneous binding of two *different* metal cations at sites n1 and n2 has so far been unclear. As for the terminology (keeping in mind also the possible different modes of coordination of the cations both to protein residues and to substrates), two-metal-ion binding may be related to *binuclear* catalysis. Thus, binding of *the same* metal cation in both sites of an active center may be related to *homobinuclear* catalysis, whereas *different* metal cations binding at the two sites of an active center may be related to *heterobinuclear* catalysis.

Preliminary comparative ^{57}Co EMS experimental studies were also performed on partly adenylylated GS from *A. brasilense* (in an intermediate adenylylation state of 44%) doped with $^{57}Co^{2+}$ alone or together with natural Mn^{2+} (the latter gives no contribution to emission spectra) [47]. Adding equimolar quantities of $^{57}Co^{2+} + Mn^{2+}$ to the metal-free enzyme, as compared to $^{57}Co^{2+}$ alone, was found to result in a partial redistribution of $^{57}Co^{II}$ between the sites, showing competitive binding of the two cations. This important finding, indirectly pointing to the possibility of heterobinuclear catalysis in bacterial GS, is in agreement with similar efficiency of the two cations in supporting the activity of partly adenylylated GS from *A. brasilense* [44]. Further ^{57}Co EMS studies are therefore warranted in order to compare not only the enzyme's specificity for different cations, but also their 'preference' for each of the two different sites (n1 and n2),

possible competitive binding, and redistribution within the GS active centers. Moreover, the coordination symmetry of $^{57}Co^{II}$ at both sites in GS from *A. brasilense* was found to be altered by changing the GS adenylylation state [47], which provides information as to the mechanism of the enzyme activity regulation by covalent modification.

17.4.5 Possibilities of ^{57}Co Substitution for Other Cations in Metalloproteins

Cobalt(II) acts as an activating cation or a cofactor in a variety of enzymes, which could thus be directly probed using ^{57}Co doping and EMS measurements. Moreover, Co^{2+} has also been shown to be applicable as an *isostructural substitute*, for example for Zn^{2+} in many zinc-containing proteins [43], and even to enhance enzyme's beneficial properties (see, for example, Refs 48,49 and references therein).

Besides the applicability of Co^{2+} as an optical (UV–Vis) probe that gives clearly different spectra for, for example, T_d and O_h coordination, $^{57}Co^{2+}$ substitution for other cations can give a highly sensitive 'snapshot' of the coordination microenvironment and its fine structural changes when used in ^{57}Co EMS. Such possibility could greatly expand the areas of ^{57}Co EMS applications beyond only cobalt-dependent metalloproteins and enzymes, greatly enhancing the importance of the technique for biochemistry, molecular biology, and related fields.

17.5 CONCLUSIONS AND OUTLOOK

In this chapter, besides an introduction to the topic and a brief consideration of earlier work, an overview is given on ^{57}Co EMS-assisted probing of the interaction of $^{57}Co^{2+}$ traces with live and dead bacterial cells in aqueous media. The Mössbauer parameters obtained in rapidly frozen suspensions of bacterial cells showed similarity for $^{57}Co^{II}$ bound to dead biomass and for $^{57}Co^{II}$ rapidly bound by the surface of live cells, reflecting the formation of similar chemical species. For live cells, however, the parameters of ^{57}Co emission spectra were found to change within an hour, which reflected ongoing metabolic transformations of the cation. The data obtained correlate with the recently discovered involvement of Co^{2+} in reactions with labile [Fe—S] clusters during their *de novo* biosynthesis or repair in *E. coli* [39], presenting the molecular basis for Co^{2+} toxicity in bacteria, besides Co^{2+}-induced oxidative stress. The results obtained show that ^{57}Co EMS can provide unique information both for speciation bioanalysis and for the monitoring of radionuclide bioleaching and its environmentally important chemical transformations mediated by soil microorganisms.

^{57}Co EMS measurements have shown for the first time that this nuclear chemistry technique is sensitive (i) to differences in the coordination of Co^{II} cations at different cation-binding sites within the enzyme active centers and (ii) to differences in the binding affinity of the sites to $^{57}Co^{II}$. Further recent studies have also revealed ^{57}Co EMS sensitivity (iii) to the effects of competitive binding of different activating cations inducing $^{57}Co^{II}$ redistribution between the sites and (iv) to fine structural changes in ^{57}Co(II) coordination induced by covalent modifications of the enzyme molecule (related to its activity regulation). The results obtained are highly promising for studying the molecular mechanisms of enzyme–substrate biospecific interactions using the unique possibilities of EMS.

ACKNOWLEDGMENTS

The author is deeply grateful to Professor Yu.D. Perfiliev and Dr L.A. Kulikov (M.V. Lomonosov Moscow State University, Moscow, Russia) as well as to Professors A. Vértes, E. Kuzmann, and Z. Homonnay (Eötvös Loránd University, Budapest, Hungary) for long-lasting collaboration, hospitality, many stimulating discussions, and their invaluable help in experimental work.

Support of the author's studies, mentioned in this chapter, from the EC (INTAS Grant 96-1015), under the NATO "Security Through Science" Program (Collaborative Linkage Grants LST.CLG.977664, LST.NR.CLG.981092, and ESP. NR.NRCLG 982857; Expert Visit Grants LST.EV.980141 and CBP.NR.NREV 981748), under the Agreements on Scientific Cooperation between the Russian and Hungarian Academies of Sciences, in particular, for 2005–2007 (Protocol, Thematic Plan, Project 37), for 2008–2010 (Protocol, Thematic Plan, Project 45), and for 2011–2013 (Protocol, Thematic Plan, Projects 28 and 29), as well as from the Russian Academy of Sciences' Commission for the Work with Young Scientists under the 6th Competition-Expertise of research projects (Grant # 205) and from the Russian Foundation for Basic Research (Grant # 13-04-01538a) is gratefully acknowledged.

REFERENCES

1. A.A. Kamnev, K. Kovács, I.V. Alenkina, M.I. Oshtrakh, this book, **2013** (Chapter 13).
2. C. Krebs, J.C. Price, J. Baldwin, L. Saleh, M.T. Green, J.M. BollingerJr., *Inorg. Chem.* **2005**, *44*, 742–757.
3. A. Vértes, D. Nagy, eds., *Mössbauer Spectroscopy of Frozen Solutions*, Akadémiai Kiadó, Budapest, **1990**.
4. D.L. Nagy, *Hyperfine Interact.* **1994**, *83*, 9–13.
5. A.A. Kamnev, *J. Mol. Struct.* **2005**, *744–747*, 161–167.
6. A. Nath, *Mössbauer Effect Ref. Data J.* **2007**, *30*, 107–109.
7. Yu.D. Perfiliev, A.A. Kamnev, *Mössbauer Effect Ref. Data J.* **2007**, *30*, 121–122.
8. Yu.D. Perfiliev, *Bull. Russ. Acad. Sci.: Phys.* **2010**, *74*, 321–325.
9. P. Gütlich, Y. Garcia, *J. Phys.: Conf. Ser.* **2010**, *217*, 012001.
10. A. Nath, *J. Nucl. Radiochem. Sci.* **2010**, *11*, A1–A3.
11. A. Nath, M.J. Prushan, J.G. Gilbert, *J. Radioanal. Nucl. Chem.* **2001**, *247*, 589–591.
12. Editor's comments, *Mössbauer Effect Ref. Data J.* **2007**, *30*, 89–90.
13. A. Vértes, L. Korecz, K. Burger, *Mössbauer Spectroscopy (Studies in Physical and Theoretical Chemistry*, Vol. 5). Elsevier/Akadémiai Kiadó, Amsterdam/Budapest, **1979**.
14. P. Hillman, H. Schechter, M. Rubinstein, *Rev. Mod. Phys.* **1964**, *36*, 360.
15. L. Robles, W.S. Rhode, C.D. Geisler, *J. Acoust. Soc. Am.* **1976**, *59*, 926–939.
16. A. Nath, M. Harpold, M.P. Klein, W. Kündig, *Chem. Phys. Lett.* **1968**, *2*, 471–476.
17. D.J. Cardin, K.N. Joblin, A.W. Johnson, G. Lang, M.F. Lappert, *Biochim. Biophys. Acta* **1974**, *371*, 44–51.
18. S. Tyagi, K. Inoue, A. Nath, *Biochim. Biophys. Acta* **1978**, *539*, 125–134.
19. T.S. Srivastava, J.L. Przybylinski, A. Nath, *Inorg. Chem.* **1974**, *13*, 1562–1564.
20. P.P. Craig, N. Sutin, *Phys. Rev. Lett.* **1963**, *11*, 460–462.
21. T.S. Srivastava, S. Tyagi, A. Nath, *Proc. Natl. Acad. Sci. USA* **1977**, *74*, 4996–5000.
22. L. Marchant, M. Sharrock, B.M. Hoffman, E. Münck, *Proc. Natl. Acad. Sci. USA* **1972**, *69*, 2396–2399.
23. A. Caubet, A. Labarta, R. Rodríguez, A. Fernandez, E. Molins, V. Moreno, J. Tejada, *Hyperfine Interact.* **1986**, *28*, 773–776.
24. A. Caubet, V. Moreno, A. Labarta, J. Tejada, *J. Inorg. Biochem.* **1990**, *39*, 173–186.
25. A. Caubet, V. Moreno, A. Labarta, J. Tejada, *Z. Naturforsch.* **1993**, *48*, 98–106.
26. E.R. Bauminger, I. Nowik, J. Yariv, *Hyperfine Interact.* **1990**, *58*, 2337–2341.
27. A.A. Kamnev, L.P. Antonyuk, V.E. Smirnova, O.B. Serebrennikova, L.A. Kulikov, Yu.D. Perfiliev, *Anal. Bioanal. Chem.* **2002**, *372*, 431–435.
28. S. Ambe, F. Ambe, T. Nozaki, *Int. J. Appl. Radiat. Isot.* **1985**, *36*, 7–11.
29. S. Ambe, *Hyperfine Interact.* **1990**, *58*, 2329–2335.
30. E. Giberman, Y. Yariv, A.J. Kalb, E.R. Bauminger, S.G. Cohen, D. Froindlich, S. Ofer, *J. Phys. Colloq.* **1974**, *35*(Suppl. 12), C6-371–C6-374.
31. A.A. Kamnev, L.P. Antonyuk, L.A. Kulikov, Yu.D. Perfiliev, *BioMetals* **2004**, *17*, 457–466.
32. A.A. Kamnev, A.V. Tugarova, L.P. Antonyuk, P.A. Tarantilis, L.A. Kulikov, Yu.D. Perfiliev, M.G. Polissiou, P.H.E. Gardiner, *Anal. Chim. Acta* **2006**, *573–574*, 445–452.
33. Yu.D. Perfiliev, V.S. Rusakov, L.A. Kulikov, A.A. Kamnev, K. Alkhatib, *J. Radioanal. Nucl. Chem.* **2005**, *266*, 557–560.
34. Yu.D. Perfiliev, V.S. Rusakov, L.A. Kulikov, A.A. Kamnev, K. Alkhatib, *Hyperfine Interact.* **2006**, *167*, 881–885.
35. V.M. Byakov, Yu.D. Perfiliev, L.A. Kulikov, S.V. Stepanov, *Mosc. Univ. Chem. Bull.* **2009**, *64*, 259–263.
36. A.A. Kamnev, Seventh International Conference on Nuclear and Radiochemistry, August 24–29, 2008, Budapest, Hungary, Book of Abstracts, **2008**, p. 48.
37. Yu.D. Perfiliev, L.A. Kulikov, L.T. Bugaenko, A.M. Babeshkin, M.I. Afanasov, *J. Inorg. Nucl. Chem.* **1976**, *38*, 2145–2148.
38. M.I. Afanasov, A.M. Babeshkin, L.A. Kulikov, Yu.D. Perfiliev, *J. Radioanal. Nucl. Chem. Lett.* **1985**, *93*, 37–42.
39. C. Ranquet, S. Ollagnier-de-Choudens, L. Loiseau, F. Barras, M. Fontecave, *J. Biol. Chem.* **2007**, *282*, 30442–30451.
40. A.A. Kamnev, A.V. Tugarova, K. Kovács, E. Kuzmann, B. Biró, P.A. Tarantilis, Z. Homonnay, *Anal. Bioanal. Chem.* **2013**, *405*, 1921–1927.
41. A.A. Kamnev, L.A. Kulikov, Yu.D. Perfiliev, L.P. Antonyuk, E. Kuzmann, A. Vértes, *Hyperfine Interact.* **2005**, *165*, 303–308.
42. A.A. Kamnev, L.P. Antonyuk, V.E. Smirnova, L.A. Kulikov, Yu.D. Perfiliev, I.A. Kudelina, E. Kuzmann, A. Vértes, *Biopolymers* **2004**, *74*, 64–68.

43. A.A. Kamnev, in *Metal Ions in Biology and Medicine*, Vol. 10, Ph. Collery, I. Maymard, T. Theophanides, L. Khassanova, T. Collery, eds., John Libbey Eurotext, Paris, **2008**, pp. 522–527.
44. L.P. Antonyuk, V.E. Smirnova, A.A. Kamnev, O.B. Serebrennikova, M.A. Vanoni, G. Zanetti, I.A. Kudelina, O.I. Sokolov, V.V. Ignatov, *BioMetals* **2001**, *14*, 13–22.
45. A.A. Kamnev, L.P. Antonyuk, L.A. Kulikov, Yu.D. Perfiliev, E. Kuzmann, A. Vértes, *Bull. Russ. Acad. Sci.: Phys.* **2005**, *69*, 1561–1565.
46. S. Yoon, S.J. Lippard, *J. Am. Chem. Soc.* **2005**, *127*, 8386–8397.
47. A.A. Kamnev, L.P. Antonyuk, V.E. Smirnova, L.A. Kulikov, Yu.D. Perfiliev, E. Kuzmann, A. Vértes, *FEBS J*. **2005**, *272* (Suppl. 1), 10.
48. E.M. Stone, E.S. Glazer, L. Chantranupong, P. Cherukuri, R.M. Breece, D.L. Tierney, S.A. Curley, B.L. Iverson, G. Georgiou, *ACS Chem. Biol.* **2010**, *5*, 333–342.
49. A. Srivastava, A.K. Sau, *IUBMB Life* **2010**, *62*, 906–915.